A hybrid radioactive and fluorescence approach is more than the sum of its parts: outcome of a phase II randomized sentinel node trial in prostate cancer patients

Wit, E.M.K.; KleinJan, G.H.; Berrens, A.C.; Vliet, R. van; Leeuwen, P.J. van; Buckle, T.; ... ; Poel, H.G. van der

European Journal of Nuclear Medicine and Molecular Imaging (2023) 50:2861–2871
https://doi.org/10.1007/s00259-023-06191-7

ORIGINAL ARTICLE

A hybrid radioactive and fluorescence approach is more than the sum of its parts; outcome of a phase II randomized sentinel node trial in prostate cancer patients

Esther M. K. Wit[1] · Gijs H. KleinJan[1,2,3] · Anne-Claire Berrens[1] · Roos van Vliet[1] · Pim J. van Leeuwen[1] · Tessa Buckle[1,2] · Maarten L. Donswijk[4] · Elise M. Bekers[5] · Fijs W. B. van Leeuwen[1,2] · Henk G. van der Poel[1,6]

Received: 6 December 2022 / Accepted: 5 March 2023 / Published online: 10 April 2023

Abstract

Objective To determine the diagnostic accuracy of the hybrid tracer indocyanine green (ICG)-Technetium-99 m(^{99m}Tc)-nanocolloid compared to sequential tracers of ^{99m}Tc-nanocolloid and free-ICG in detecting tumor-positive lymph nodes (LN) during primary surgery in prostate cancer (PCa) patients.

Introduction Image-guided surgery strategies can help visualize individual lymphatic drainage patterns and sentinel lymph nodes (SLNs) in PCa patients. For lymphatic mapping radioactive, fluorescent and hybrid tracers are being clinically exploited. In this prospective randomized phase II trial, we made a head-to-head comparison between ICG-^{99m}Tc-nanocolloid (hybrid group) and ^{99m}Tc-nanocolloid and subsequent free-ICG injection (sequential group).

Methods PCa patients with a >5% risk of lymphatic involvement according to the 2012 Briganti nomogram and planned for prostatectomy were included and randomized (1:1) between ultrasound-guided intraprostatic tracer administration of ICG-^{99m}Tc-nanocolloid ($n=69$) or ^{99m}Tc-nanocolloid ($n=69$) 5 h before surgery. Preoperative lymphoscintigraphy and SPECT/CT were performed to define the locations of the SLNs. Additionally, all participants in the sequential group received an injection of free-ICG at time of surgery. Subsequently, all (S)LNs were dissected using fluorescence guidance followed by an extended pelvic lymph node dissection (ePLND). The primary outcome was the total number of surgically removed (S)LNs and tumor-positive (S)LNs.

Results The total number of surgically removed (S)LN packages was 701 and 733 in the hybrid and sequential groups, respectively ($p=0.727$). The total number of fluorescent LNs retrieved was 310 and 665 nodes in the hybrid and sequential groups, respectively ($p<0.001$). However, no statistically significant difference was observed in the corresponding number of tumor-positive nodes among the groups (44 vs. 33; $p=0.470$). Consequently, the rate of tumor-positive fluorescent LNs was higher in the hybrid group (7.4%) compared to the sequential group (2.6%; $p=0.002$), indicating an enhanced positive predictive value for the hybrid approach. There was no difference in complications within 90 days after surgery ($p=0.78$).

Conclusions The hybrid tracer ICG-^{99m}Tc-nanocolloid improved the positive predictive value for tumor-bearing LNs while minimizing the number of fluorescent nodes compared to the sequential tracer approach. Consequently, the hybrid tracer ICG-^{99m}Tc-nanocolloid enables the most reliable and minimal invasive method for LN staging in PCa patients.

Keywords Prostate cancer · Sentinel lymph node · Image-guided surgery · Lymphadenectomy · Robot-assisted radical prostatectomy · Hybrid tracer · Indocyanine

Introduction

One of the most elaborately studied surgical procedures that benefits from image guidance is the so-called sentinel lymph node (SLN) procedure. During this procedure, lymphatic flow from a primary tumor is visualized using lymphangiographic agents (e.g., methylene blue, fluorescein, or indocyanine green (ICG) [1–3]) and/or node-accumulating

This article is part of the Topical Collection on Oncology - Genitourinary

✉ Esther M. K. Wit
e.wit@nki.nl

Extended author information available on the last page of the article

imaging agents, so-called SLN tracers (radiocolloids such as Technetium-99 m (^{99m}Tc)-nanocolloid) [4–6]. Lymphangiographic agents can be used to rapidly stain draining lymphatic templates due to their "small" size and rapid migration kinetics. On the other hand, node-accumulating agents allow careful classification of sequential drainage patterns [7, 8]. Despite these fundamental differences in tracer kinetics, both approaches are employed during SLN procedures.

Their proven ability to prevent extensive nodal dissections has made SLN procedures standard of care for clinically node-negative breast cancer and melanoma patients [9, 10]. The procedure is also being put forward as a valid treatment option in vulvar, cervical, and penile cancer [11–14] and has been extensively explored in a wide variety of cancers, among which prostate cancer (PCa). As early as 1999, Wawroschek et al. reported on the validity of radio-guided SLN procedures in PCa patients, who incorporated preoperative nuclear imaging with intraoperative gamma tracing [15]. Their pioneering work indicated that the procedure has also the potential to reduce perioperative morbidity and may increase the sensitivity of the detection of micrometastases. With the rise of robotic surgery, traditional gamma probes became difficult to implement and laparoscopic near-infrared (NIR) fluorescence imaging started to take over as leading intraoperative guidance modality [7].

The SLN procedures in PCa essentially evolved towards two approaches: (1) use of ICG-^{99m}Tc-nanocolloid (a fully integrated (hybrid) tracer entity whereby the SLNs are both radioactive and fluorescent) [7] and (2) the multi-step implementation of ^{99m}Tc-nanocolloid as SLN agent combined with free-ICG as lymphoscintigraphic agent (sequential tracer approach) [16]. In both cases, preoperative lymphoscintigraphy including single photon emission computed tomography with low-dose computed tomography (SPECT/CT) provides the operating surgeon with a roadmap, which is a valuable addition that indicates the anatomical location of the SLN and helps to plan the intervention accordingly [17]. A multitude of SLN studies in PCa, using either ^{99m}Tc-nanocolloid or ICG-^{99m}Tc-nanocolloid tracer, has indicated that the SLN procedure is a reliable diagnostic procedure for nodal staging with high sensitivity and specificity rates [18–26]. Logistical reasons, but also the fact that not every medical center has a highly skilled nuclear medicine department, lead to the suggestion that intraoperative fluorescence imaging can possibly replace the preoperatively radiocolloid-based method. Six groups reporting use of free-ICG (0.5–2 mg/patient) indicated that fluorescence detection proved highly sensitive but relatively nonspecific for disease [27–33]. While using ICG-^{99m}Tc-nanocolloid means a substantially lower amount of ICG is injected (0.25 mg/patient), thus making detection potentially more challenging, the procedure is claimed to yield an increased SLN specificity [26]. A systematic comparison between the use of ICG-^{99m}Tc-nanocolloid and free-ICG in PCa, however, has only taken place in pre-clinical studies [34].

To provide a head-to-head comparison between the use of ICG-^{99m}Tc-nanocolloid and a cocktail of separately injected ^{99m}Tc-nanocolloid and free-ICG approach, we conducted a phase II randomized trial in PCa patients. Here, we focused on determining the number of nodes harvested with fluorescence guidance and the positive predictive value for tumor-positive LNs.

Methods

Patients

Eligible patients with histopathologically proven PCa, that were clinically N0M0 on preoperative imaging (PET/CT and/or bone scan), had a risk of nodal metastases of >5% according to the 2012 Briganti nomogram, and were scheduled for a robot-assisted radical prostatectomy (RARP) with extended pelvic lymph node dissection (ePLND), were included in this prospective randomized study. Exclusion criteria were history of iodine allergy, hyperthyroid or thyroidal adenoma, and kidney insufficiency. Patients were randomly allocated 1:1 to the hybrid tracer or sequential tracer group. ICG-^{99m}Tc-nanocolloid (250 µg ICG combined 200 MBq ^{99m}Tc-nanocolloid in 2 mL) or ^{99m}Tc-nanocolloid (200 MBq ^{99m}Tc-nanocolloid in 2 mL) was administered approximately 5 h prior to surgery in 4 deposits of 0.5 mL into the peripheral zone of the prostate using transrectal ultrasound (TRUS) guiding. Before incision and docking of the robot, patients allocated to the sequential group were separately administered 2 mL ICG (10 mg) in 2 deposits of 1 mL directed towards the peripheral zone of the prostate (Fig. 1).

This phase II randomized controlled trial was approved by the local Ethic Committee and registered as the M13PSN study with registration number NL46580.031.13. Written informed consent was obtained from all patients prior to the received treatment.

Preoperative SLN imaging

Following tracer injection, lymphatic mapping was performed using static planar lymphoscintigraphy of the pelvic area (15 min and 2 h post-injection) followed by SPECT/CT using a dual head gamma camera (Symbia T, Siemens, Erlangen, Germany), similar in both arms of the study. Planar images and SPECT, CT, and fused SPECT/CT including volume-rendering reconstructions were displayed using OsiriX medical imaging software (Pixmeo, Geneva, Switzerland). The images were interpreted and hotspots were assigned as SLNs or higher echelon nodes by an experienced

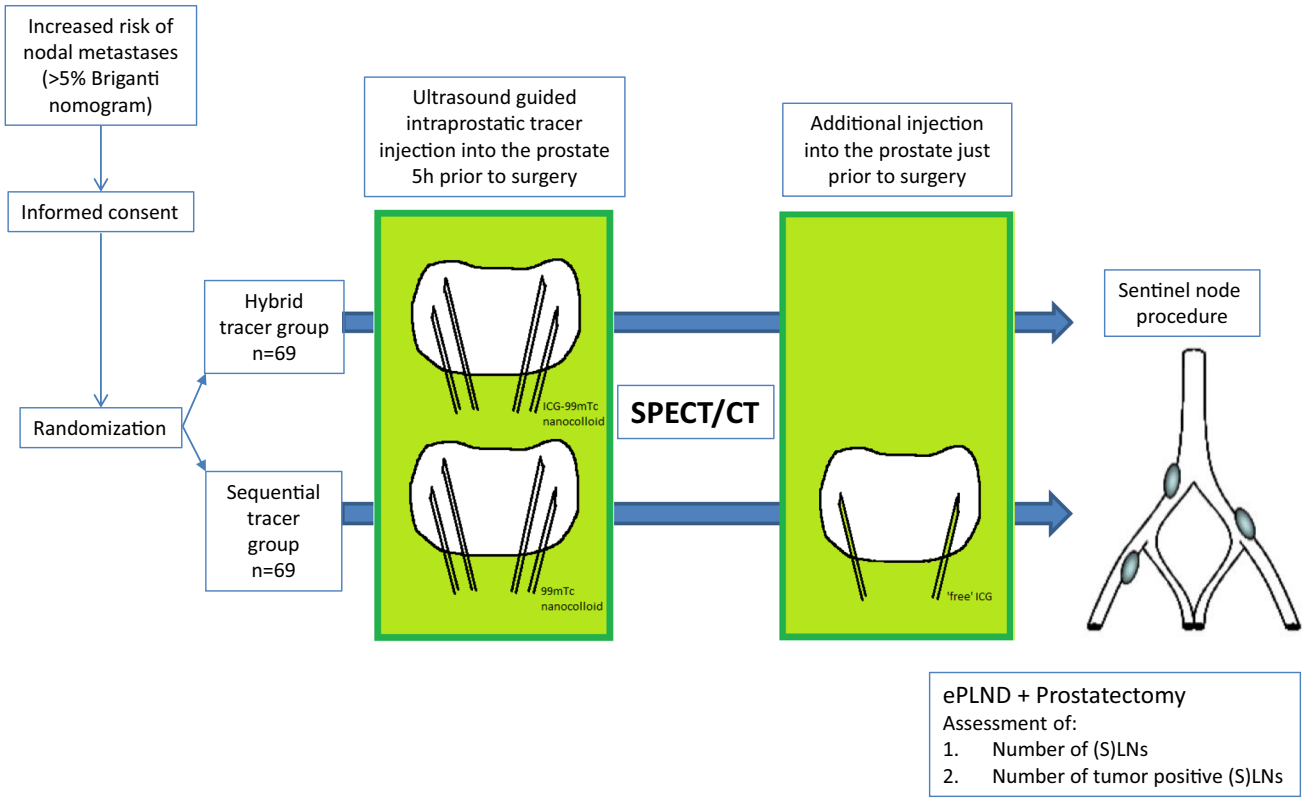

Fig. 1 Flow chart of the study

nuclear medicine physician. An earlier study describes the protocol in detail [35].

Surgical procedure

Prostatectomy and nodal sampling were performed by three surgeons experienced in robot-assisted surgery using a Firefly fluorescence endoscope equipped da Vinci Si surgical system (Intuitive surgical, Sunnyvale, CA, USA). Fused axial SPECT/CT images were used as roadmap to indicate the anatomical localization of hotspots and were displayed in the operating room to enable easy consultation by the operating surgeon. During surgery, the nodal fluorescence was identified using the Firefly camera's fluorescence imaging mode of the da Vinci Si surgical system (Fig. 2). Hereby, a SLN package was defined as a surgically resected specimen that can contain multiple LNs. After removal of the nodes, the radioactive counts in LNs were determined ex vivo at the operating table with a laparoscopic gamma probe (Europrobe 2; Eurorad, Eckbolsheim, France). In this way, SLNs that were not detected by fluorescence intraoperatively were still labeled as SLNs for pathological assessment based on their radioactivity. The removed nodes were correlated with location of the SLNs on SPECT/CT imaging.

Following identification of fluorescent LNs and their subsequent removal, a complementary ePLND was performed, followed by a RARP, in that order. The ePLND template consisted of the common iliac artery, cranially confined by the ureteric crossing; the internal iliac vessels and the obturator fossa and external iliac vessels, caudally confined by the deep circumflex vein and femoral canal. The lateral border was the genitofemoral nerve and the medial border the peri-vesical fat.

Pathology

Excised fluorescent and radioactive LN packages were labeled as SLNs and as such fixed in formaldehyde and subsequently cut in 2-mm-thick slices perpendicular to the long axis. They were embedded in paraffin prior to serial sectioning in 3 slides at 200 µm intervals. All slides were stained with hematoxylin and eosin (H&E) staining and the middle slide was additionally stained with a pancytokeratin staining. Non-fluorescent and/or radioactive LNs were cut in 3-mm slices, usually longitudinal to the long axis, and only one H&E slide per block was made. Pathological assessment was performed by an experienced uropathologist specialized in PCa.

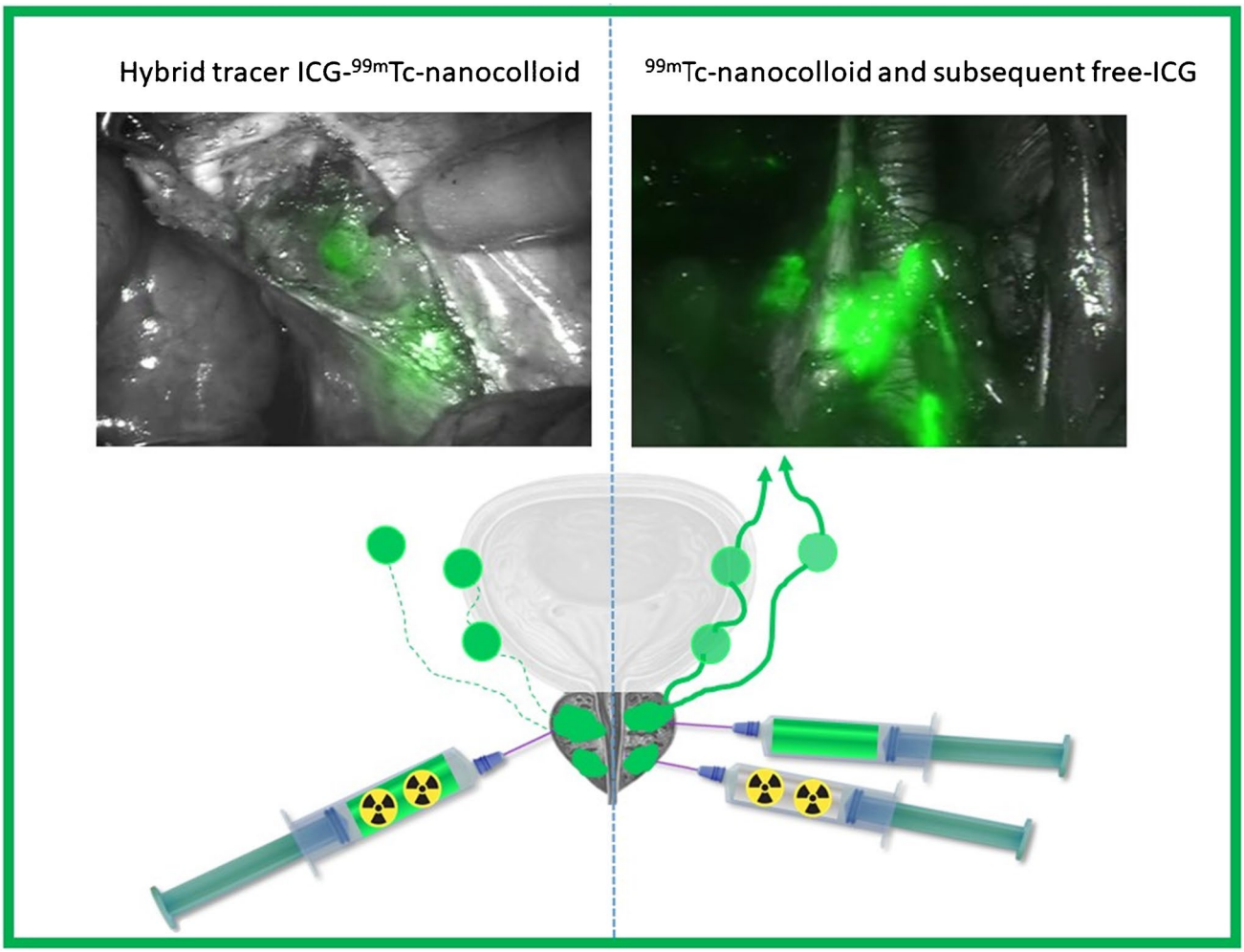

Fig. 2 Intraoperative view of nodal fluorescence using the Firefly camera's fluorescence imaging mode of the da Vinci surgical system, showing a moderate fluorescent signal in accumulating lymph nodes with the hybrid approach (left side), compared to intense fluorescence in nodes and lymphatic vessels with the free-ICG tracer (right side)

Indications where the image guidance procedure failed were defined as nodal metastases not residing in the resected SLN packages, but elsewhere in the ePLND templates.

Complications and follow-up

Intra- and postoperative complications (within 90 days after surgery) were scored using the Clavien-Dindo score [36]. Secondary endpoints were biochemical-free survival (BFS) and metastasis-free survival (MFS). Because MFS is considered a validated surrogate endpoint for overall survival in localized PCa [37], patients were evaluated for MFS of 2–8 year follow-up data. BFS was defined as the time between randomization and a PSA level >0.2 ng/ml after RARP. MFS was defined as the time between randomization and the appearance of a metastatic recurrence (any N1 and/or M1) as suggested by bone scintigraphy, CT, or PSMA PET/CT.

Statistics

The rate in the number of tumor-positive SLNs was used to calculate the sample size. In an analysis from an earlier SLN study using ICG-^{99m}Tc-nanocolloid, we detected a median of 3 SLNs per patient [7]; a free-ICG study from the Salzburg group identified a median of 10 SLNs [28]. The number of tumor-positive SLNs was 12% vs. 15%, respectively. To test which tracer results in the highest yield of tumor-positive LNs, with an 80% power, statistics indicated we needed to include 69 patients in both study arms. For continuous variables, normality of distribution was verified using the Kolmogorov-Smirnov test. For variables that had no normal distribution, the nonparametric Mann-Whitney *U* test was used. For binomial variables that had normal distribution, the chi-square and Fisher's exact test were used. Kaplan-Meier curves using log-rank rest were generated for BFS and MFS analyses. *p*-values <0.05 were considered significant.

Statistical analysis was performed using SPSS version 27 (IBM).

Results

Patients

From August 2014 to March 2020, a total of 138 patients underwent randomization, 69 were assigned to the hybrid group and 69 to the sequential group. Demographic and disease characteristics were well balanced between the two groups (Table 1). Median follow-up was 42 months (IQR 26.8–54.3).

Preoperative imaging findings

The median number of SLNs identified on SPECT/CT did not differ between the two groups (3 vs. 4, $p=0.511$). Absence of drainage (i.e., bilateral non-visualization) occurred in 2 patients (2.9%) in the hybrid group and 3 patients (4.3%) in the sequential group (Table 2). Respectively 14 (20.3%) and 10 (14.5%) patients had unilateral visualization on SPECT/CT imaging.

Intraoperative findings

The time interval between radionuclide tracer injection and surgery was similar for both groups (5:15 h (hybrid group) vs. 5:17 h (sequential group), $p=0.941$; Table 3). The median number of total removed (S)LN packages was comparable between the two groups (10 vs. 10, $p=0.139$; Table 3).

Some SLNs on SPECT/CT imaging were surgically not pursued due to inaccessible locations, 55 (hybrid tracer) vs. 74 (sequential tracer; $p=0.472$), resulting in the SPECT/CT directed resection of 177 (hybrid tracer) vs. 190 (sequential tracer; $p=0.442$) SLN packages (Table 3). It is known that intraoperative fluorescence imaging during SLN procedures can be relatively insensitive, making confirmative back table fluorescence imaging and gamma probe measurements essential [35, 38]. Real-time intraoperative fluorescent

Table 1 Prostate cancer patient characteristics indicated as median values (Median) with interquartile range (IQR)

	Hybrid group ($n=69$)	Sequential group ($n=69$)	p-value
Age at surgery (years) Median (IQR)	67 (59.0–70.5)	69 (63.0–71.5)	$p=0.694$
PSA at diagnosis (ng/ml) Median (IQR)	10.3 (7.8–17.2)	8.9 (6.9–13.5)	$p=0.457$
Clinical stage (%)			
cT1	11 (15.9%)	12 (17.4%)	$p=0.856$
cT2	41 (59.4%)	35 (50.7%)	
cT3	17 (24.6%)	22 (31.9%)	
Biopsy Gleason sum (%)			
6	1 (1.4%)	2 (2.9%)	$p=0.858$
7	46 (66.7%)	44 (63.8%)	
8–10	22 (31.9%)	23 (33.3%)	
Prostate volume (ml) Median (IQR)	40 (32–54)	40 (30–58)	$p=0.664$
Briganti score 2012 Median (IQR)	14.0 (8.7–34.3)	16.0 (8.9–33.4)	$p=0.603$

IQR interquartile range, *ng* nanogram, *ml* milliliter

Table 2 Preoperative imaging findings. Results are indicated as median values (Median) with interquartile range (IQR)

	Hybrid group ($n=69$)	Sequential group ($n=69$)	p-value
Administered dose in MBq Median (IQR)	209.9 (194.0–219.1)	206.3 (194.4–216.9)	$p=0.735$
Bilateral non-visualization	2 (2.9%)	3 (4.3%)	$p=0.208$
Total number of SLNs on SPECT/CT Median (IQR)	232 3 (2.0–4.5)	264 4 (2.0–5.0)	$p=0.511$

MBq megabecquerel, *IQR* interquartile range, *SLN* sentinel lymph node, *SPECT/CT* single photon emission computed tomography/computed tomography

Table 3 Intraoperative findings. Results are indicated as median values (Median) with interquartile range (IQR)

		Hybrid group ($n=69$)	Sequential group ($n=69$)	p-value
Interval between injection and surgery (hours) Median (IQR)		5:15 (4:22–5:32)	5:17 (4:42–5:45)	$p=0.941$
Duration of surgery (hours) Median (IQR)		2:29 (2:04–2:45)	2:20 (2:05–2:46)	$p=0.654$
Resected SLNs seen on SPECT/CT Median (IQR)		177 2 (1–4)	190 3 (1–4)	$p=0.442$
Inaccessible SLNs not resected Median (IQR)		55 0 (0–1)	74 1 (0–2)	$p=0.472$
Fluorescent SLN packages, correlated with radioactive SLNs on SPECT/CT	Yes	92 (52%)	145 (76%)	$p<0.001$
	No	70	29	
	Unknown	15	16	
Radioactive SLN packages on SPECT/CT	Yes	166 (94%)	174 (92%)	$p=0.923$
	No	2	2	
	Unknown	9	14	
Total fluorescent (S)LN packages Median (IQR)		160 2 (0–4)	361 5 (2–8)	$p<0.001$
Total radioactive (S)LN packages Median (IQR)		351 4 (3–7)	388 5 (4–8)	$p=0.306$
Total number of resected (S)LN packages Median (IQR)		701 10 (8–12)	733 10 (9–13)	$p=0.139$

IQR interquartile range, *SLN* sentinel lymph node, *SPECT/CT* single photon emission computed tomography/computed tomography

nodal identification rates of SLN packages were 52% (hybrid group) and 76% (sequential group), respectively ($p<0.001$). The other SLN packages were identified by back table specimen analyses. The ex vivo radioactive SLN packages on SPECT/CT imaging did not differ between the two groups (94% (hybrid group) vs. 92% (sequential group); Table 3). In both groups, the distribution of resected fluorescent LN packages—within or outside ePLND template—was similar (Table 4). Duration of surgery (2:29 h (hybrid tracer) vs. 2:20 h (sequential tracer), $p=0.654$) was again similar (Table 3).

Pathologic examination

The median number of resected LNs per patient (SLN+ePLND = 20 vs. 21; $p=0.727$) and the total number of LN metastases (44 vs 33; $p=0.470$) were comparable for both groups (Table 5). In the hybrid group, the amount of nodes resected by image guidance was halved (310 vs 665; $p<0.001$; Table 5). Interestingly, 7.4% of the fluorescent nodes with the hybrid approach yielded metastases, whereas only 2.6% of the fluorescent nodes from the sequential group contained metastases ($p=0.002$; Table 5). This indicates a threefold increase in positive predictive value for the former. The percentage fluorescent node-positive SLNs, correlated with the location of radioactive SLNs on SPECT/CT, was comparable for both groups (68% (hybrid group) vs. 61% (sequential group; $p=0.22$). The same was true for indications where image guidance failed (1.4% vs. 1.4%, respectively).

Complications and follow-up

Overall, complication rate within 90 days after surgery was 30.4%, of which 18.1% were Clavien-Dindo grade III/IV complications. No significant differences were found between both groups for incidence (29.0% vs. 31.9%, $p=0.78$; Table 6) or Clavien-Dindo severity score of complications. Focusing on complications related to SLN and ePLND (lymphedema, lymphocele, thrombo-embolic events, iatrogenic ureter lesion), these complication rates were again not significantly different (8.7% vs. 11.6%, $p=0.57$).

With a median follow-up of 42 months (IQR 26.8–54.3), the median BFS was 31.0 months in the hybrid group and 32.0 months in the sequential group ($p=0.73$). Subsequently, the median MFS was 38.0 and 39.0 months in the hybrid- and sequential group, respectively ($p=0.38$).

Discussion

By performing a randomized trial, we have been able to unravel the clinical impact of relying on the intraoperative fluorescence guidance provided by the hybrid tracer

Table 4 Surgical location of fluorescent (S)LN packages

	Hybrid group ($n=69$)	Sequential group ($n=69$)	p-value
Obturator fossa	75 (46.9%)	131 (36.3%)	
Internal iliac artery	9 (5.6%)	19 (5.3%)	
External iliac artery	31 (19.4%)	87 (24.1%)	
Cloquet	2 (1.3%)	7 (1.9%)	
Presacral area	3 (1.9%)	24 (6.6%)	
Preprostatic fatty tissue	1 (0.6%)	5 (1.4%)	
Paravesical area	2 (1.3%)	15 (4.2%)	
Pararectal area	11 (6.9%)	16 (4.4%)	
Umbilical ligament	13 (8.1%)	22 (6.1%)	
Common iliac artery	8 (5.0%)	4 (1.1%)	
Marcille triangle	2 (1.3%)	21 (5.8%)	
Other	3 (1.9%)	9 (2.5%)	
Unknown	0 (0%)	1 (0.3%)	
Total number of fluorescent packages within ePLND	119 (74.4%)	266 (73.7%)	$p=0.914$
Total number of fluorescent packages outside ePLND	41 (25.6%)	95 (26.1%)	
Total fluorescent (S)LN packages	160	361	$p<0.001$
Total number of resected (S)LN packages	701	733	$p=0.139$

ePLND extended pelvic lymph node dissection, *SLN* sentinel lymph node

Table 5 Pathological findings. Characteristics are indicated as median values (Median) with interquartile range (IQR)

	Hybrid group ($n=69$)	Sequential group ($n=69$)	p-value
LN metastases (% patients)			
yes	21 (30.4%)	18 (26.1%)	$p=0.262$
no	48 (69.6%)	51 (73.9%)	
Pathological stage (%)			
pT2	33 (47.8%)	34 (49.3%)	$p=0.521$
pT3	34 (49.3%)	35 (50.7%)	
pT4	2 (2.9%)	0 (0%)	
Pathological Gleason sum (%)			
6	4 (5.8%)	0 (0%)	$p=0.157$
7	50 (72.5%)	50 (72.5%)	
8–10	15 (21.7%)	19 (27.5%)	
Total number of LNs investigated	1523	1482	
Median (IQR)	20 (16.5–28.5)	21 (14.0–25.0)	$p=0.727$
Total number of LN metastases identified	44 (2.9%)	33 (2.2%)	
Median (IQR)	0 (0–1)	0 (0–1)	$p=0.470$
Total number of LNs recovered from fluorescent packages	310	665	$p<0.001$
Median (IQR)	3 (0–7)	8 (3–15.5)	
Fluorescent tumor-positive LNs	23 (7.4%)	17 (2.6%)	$p=0.002$
Median (IQR)	0 (0–1)	0 (0–1)	
Failure image guidance	1 (1.4%)	1 (1.4%)	$p=1.000$

IQR interquartile range, *SLN* sentinel lymph node, *SPECT/CT* single photon emission computed tomography/computed tomography

ICG-^{99m}Tc-nanocolloid (a SLN specific agent) versus the fluorescence guidance provided by free-ICG (a lymphangiographic agent). Since the procedures were performed combined with an ePLND, there were no differences in the total number of resected (S)LNs or histologically positive (S)LNs. Looking at the LNs resected under fluorescence guidance, the hybrid tracer decreased the fluorescence-based harvesting twofold, while increasing the chance

Table 6 Complications within 90 days after surgery, using the Clavien-Dindo score

	Hybrid group ($n=69$)	Sequential group ($n=69$)	p-value
Patients with complications	20 (29.0%)	22 (31.9%)	$p=0.78$
Total number of complications	25	25	$p=0.42$
Clavien-Dindo I	2	3	$p=0.29$
- Lymph edema	1	3	
- Neuropraxia n.obturatorius	1	0	
Clavien-Dindo II	10	10	$p=0.33$
- Arithmia	1	0	
- Pneumonia	1	1	
- Pulmonary embolism	1	0	
- Urosepsis	2	3	
- Sclerosis anastomosis	0	1	
- Pain legs e.c.i	1	1	
- UTI	2	2	
- DVT	0	2	
- Urinary leakage	2	0	
Clavien-Dindo IIIa	9	8	$p=0.43$
- Lymphocele (drainage)	3	2	
- Urinoma (drainage)	1	0	
- Urinary retention (CAD/SPC)	1	4	
- LUTS	0	1	
- Urinary leakage (CAD/NSK/occlusion)	3	1	
- CIC for stricture	1	0	
Clavien-Dindo IIIb	4	3	$p=0.32$
- Correction inguinal hernia	1	1	
- Correction cicatricial hernia	2	0	
- Laparotomy for bowel perforation	0	1	
- Iatrogenic ureter transsection	0	1	
- Reanastomosis urinary leakage	1	0	
Clavien-Dindo IVa	0	1	$p=0.42$
- Trachea occlusion	0	1	

UTI urinary tract infection, *DVT* deep venous thrombosis, *CAD* catheter a demeure, *SPC* suprapubic catheter, *LUTS* lower urinary tract symptoms, *NSK* nephrostomy catheter, *CIC* clean intermittent catheterization

of identifying tumor-bearing LNs using fluorescence threefold.

As the radiocolloid concentration and amount of radioactive activity were similar for both groups, no difference was seen on SPECT/CT. Both the total number of SLNs and the SLNs with aberrant drainage patterns were similar. This corresponds to the findings of Brouwer et al., who concluded that the lymphatic drainage pattern of ICG-^{99m}Tc-nanocolloid is identical to that of ^{99m}Tc-nanocolloid on SPECT/CT [39]. Several studies comparing free-ICG with ^{99m}Tc-nanocolloid, e.g., in early stage cervical and vulvar cancer [40–42], underscore discrepancies in behavior between the two agents. In our study, use of free-ICG meant a 40 times higher quantity of fluorescent dye was injected as compared to that used in ICG-^{99m}Tc-nanocolloid (10 mg vs 250 µg), whereby free-ICG can be considered lymphangiographic agent and ICG-^{99m}Tc-nanocolloid a SLN specific agent. We observed that the sequential group yielded more than twofold increase in the number of fluorescent packages resected. The general assumption is that increasing the amount of resected LNs converts to increasing the chance of harvesting more histologically positive LNs ("more is better"). Our current finding shed doubt on the validity of this approach and perhaps even indicates "less is more." While the overall tumor recovery rates were similar, intraoperative ICG fluorescence in the sequential group was about 3 times less likely to indicate the presence of tumor than in the hybrid group, thus making the hybrid approach the more tumor specific of the two and with that the more accurate image guidance approach.

In fluorescence-guided surgery, signal intensity and in particular the signal to background ratio drive surgical decision-making [43]. In our study, the complex pelvic anatomy and the fact that a less sensitive laparoscopic

fluorescence camera was used [44] meant that real-time in vivo fluorescence detection percentage were relatively low for both groups, 53% (hybrid group) and 76% (sequential group; $p < 0.001$), percentages that are substantially lower than our previous reports [35, 45], underlining how critical back table analyses are for these procedures. In addition, gamma tracing of the radioactive signal provided a valuable back-up for lesions with low fluorescence intensity [46]. The fact that real-time fluorescence imaging can already be challenging in SLN procedures raises concerns for the pursuit of receptor-target image-guided surgery procedures for, e.g., the prostate-specific membrane antigen (PSMA) [47] and other future fluorescence-guided surgery applications wherein the amount of tracer accumulated in target lesions will be relatively low [38], a setting where hybrid approaches that allow for the back-up by gamma tracing could even be more critical.

This study comes with some limitations. To accurately compare the impact of ICG-^{99m}Tc-nanocolloid and free-ICG on the surgical resection, we send all intraoperative fluorescent and/or radioactive nodes to pathology as SLNs. While this facilitates the comparison between the groups, it deviates from the concept that SLNs are only the nodes designated as SLNs in the SPECT/CT images [48]. Critics may state that the multi-step use of ^{99m}Tc-nanocolloid and free-ICG, while greatly over sampling the SLNs, yielded similar pathological findings without adding complications. This argument, however, fails to consider the use of free-ICG doubled the pathological workload; SLNs are more meticulously examined. In general, the SLN concept is poised as a diagnostic tool, with the aim to reduce complications by minimizing the nodal harvesting, while retaining diagnostic accuracy [26]. This only seems to be the case for the hybrid approach, but as we performed the SLN concept in conjunction with an ePLND, the benefit of having the ePLND as control meant we were not able to reduce nodal harvesting with either technology. As a result, the amount of healthy LNs that has been resected during this study was relatively high (97.1% (hybrid group) vs. 97.8% (sequential group)). The limited utility of the rigid laparoscopic gamma probe in the robotic setting hampering its application in small-pelvis robot surgery meant radioguidance was not regularly used in vivo. The recent availability of the robot-tailored DROP-IN gamma probe may change this for future studies [49], highlighting the importance of multidisciplinary collaboration to achieve the best outcomes for PCa patients [50]. Finally, recent literature indicates that the positive predictive value of the SLN procedure can be increased by applying intratumoral, rather than peripheral hybrid tracer administration [51].

Conclusion

This study clearly indicates that the composition wherein ICG is used greatly impacts the fluorescence guidance aspect of SLN procedures. The hybrid ICG-^{99m}Tc-nanocolloid approach halved the number of LNs harvested under fluorescence guidance, while increasing the positive predictive value of the procedure by a factor of three. As a result, the hybrid tracer ICG-^{99m}Tc-nanocolloid enables the most reliable and minimal invasive method for LN staging in PCa patients.

Funding This work was partially supported by an ERC starting grant (2012–306890) and a NWO-TTW-VICI grant (TTW 16141).

References

1. Peek MC, Charalampoudis P, Anninga B, Baker R, Douek M. Blue dye for identification of sentinel nodes in breast cancer and malignant melanoma: a systematic review and meta-analysis. Future Oncol. 2017;13(5):455–67.
2. Valiveru RC, Agarwal G, Agrawal V, Gambhir S, Mayilvaganan S, Chand G, et al. Low-cost fluorescein as an alternative to radio-colloid for sentinel lymph node biopsy-a prospective validation study in early breast cancer. World J Surg. 2020;44(10):3417–22.
3. Guo J, Yang H, Wang S, Cao Y, Liu M, Xie F, et al. Comparison of sentinel lymph node biopsy guided by indocyanine green, blue dye, and their combination in breast cancer patients: a prospective cohort study. World J Surg Oncol. 2017;15(1):196.
4. Brouwer OR, van den Berg NS, Matheron HM, van der Poel HG, van Rhijn BW, Bex A, et al. A hybrid radioactive and fluorescent tracer for sentinel node biopsy in penile carcinoma as a potential replacement for blue dye. Eur Urol. 2014;65(3):600–9.
5. Papadia A, Gasparri ML, Buda A, Mueller MD. Sentinel lymph node mapping in endometrial cancer: comparison of fluorescence dye with traditional radiocolloid and blue. J Cancer Res Clin Oncol. 2017;143(10):2039–48.
6. Van Den Berg NS, Buckle T, Kleinjan GI, Klop WM, Horenblas S, Van Der Poel HG, et al. Hybrid tracers for sentinel node biopsy. The quarterly journal of nuclear medicine and molecular imaging : official publication of the Italian Association of Nuclear Medicine (AIMN) [and] the International Association of Radiopharmacology (IAR), [and] Section of the So. 2014;58(2):193–206.
7. van der Poel HG, Buckle T, Brouwer OR, Valdes Olmos RA, van Leeuwen FW. Intraoperative laparoscopic fluorescence guidance to the sentinel lymph node in prostate cancer patients: clinical proof of concept of an integrated functional imaging approach using a multimodal tracer. Eur Urol. 2011;60(4):826–33.
8. van den Berg NS, Valdes-Olmos RA, van der Poel HG, van Leeuwen FW. Sentinel lymph node biopsy for prostate cancer: a hybrid approach. J Nucl Med Off Publ Soc Nucl Med. 2013;54(4):493–6.
9. Mok CW, Tan SM, Zheng Q, Shi L. Network meta-analysis of novel and conventional sentinel lymph node biopsy techniques in breast cancer. BJS Open. 2019;3(4):445–52.
10. Quartuccio N, Siracusa M, Pappalardo M, Arnone A, Arnone G. Sentinel node identification in melanoma: current clinical

impact, new emerging SPECT radiotracers and technological advancements. An update of the last decade. Curr Radiopharm. 2020;13(1):32–41.
11. Collarino A, Fuoco V, Garganese G, Pereira Arias-Bouda LM, Perotti G, Manca G, et al. Lymphoscintigraphy and sentinel lymph node biopsy in vulvar carcinoma: update from a European expert panel. Eur J Nucl Med Mol Imaging. 2020;47(5):1261–74.
12. Giammarile F, Bozkurt MF, Cibula D, Pahisa J, Oyen WJ, Paredes P, et al. The EANM clinical and technical guidelines for lymphoscintigraphy and sentinel node localization in gynaecological cancers. Eur J Nucl Med Mol Imaging. 2014;41(7):1463–77.
13. Wever L, de Vries HM, van der Poel H, van Leeuwen F, Horenblas S, Brouwer O. Minimally invasive evaluation of the clinically negative inguinal node in penile cancer: dynamic sentinel node biopsy. Urol Oncol. 2022;40(6):209–14.
14. Jewell EL, Huang JJ, Abu-Rustum NR, Gardner GJ, Brown CL, Sonoda Y, et al. Detection of sentinel lymph nodes in minimally invasive surgery using indocyanine green and near-infrared fluorescence imaging for uterine and cervical malignancies. Gynecol Oncol. 2014;133(2):274–7.
15. Wawroschek F, Vogt H, Weckermann D, Wagner T, Harzmann R. The sentinel lymph node concept in prostate cancer - first results of gamma probe-guided sentinel lymph node identification. Eur Urol. 1999;36(6):595–600.
16. Jeschke S, Lusuardi L, Myatt A, Hruby S, Janetschek G. Lymph node pathway visualization in real time by laparoscopic radioisotope-and fluorescence-guided sentinel lymph node dissection in prostate cancer staging. European Urology, Supplements. 2012;11 (1):e1009-ea.
17. Vermeeren L, Valdes Olmos RA, Meinhardt W, Bex A, Van Der Poel HG, Vogel WV, et al. Value of SPECT/CT for detection and anatomic localization of sentinel lymph nodes before laparoscopic sentinel node lymphadenectomy in prostate carcinoma. J Nucl Med. 2009;50(6):865–70.
18. Holl G, Dorn R, Wengenmair H, Weckermann D, Sciuk J. Validation of sentinel lymph node dissection in prostate cancer: experience in more than 2,000 patients. Eur J Nucl Med Mol Imaging. 2009;36(9):1377–82.
19. Van den Bergh L, Joniau S, Haustermans K, Deroose CM, Isebaert S, Oyen R, et al. Reliability of sentinel node procedure for lymph node staging in prostate cancer patients at high risk for lymph node involvement. Acta Oncol (Stockholm, Sweden). 2015;54(6):896–902.
20. Brenot-Rossi I, Rossi D, Esterni B, Brunelle S, Chuto G, Bastide C. Radioguided sentinel lymph node dissection in patients with localised prostate carcinoma: influence of the dose of radiolabelled colloid to avoid failure of the procedure. Eur J Nucl Med Mol Imaging. 2008;35(1):32–8.
21. Meinhardt W, Valdes Olmos RA, Van Der Poel HG, Bex A, Horenblas S. Laparoscopic sentinel node dissection for prostate carcinoma: technical and anatomical observations. BJU Int. 2008;102(6):714–7.
22. Muck A, Langesberg C, Mugler M, Rahnenfuhrer J, Wullich B, Schafhauser W. Clinical outcome of patients with lymph node-positive prostate cancer following radical prostatectomy and extended sentinel lymph node dissection. Urol Int 2015; 94(3):296–306.
23. Ponholzer A, Lamche M, Klitsch M, Kraischits N, Hiess M, Schenner M, et al. Sentinel lymphadenectomy compared to extended lymphadenectomy in men with prostate cancer undergoing prostatectomy. Anticancer Res. 2012;32(3):1033–6.
24. Stanik M, Capak I, Macik D, Vasina J, Lzicarova E, Jarkovsky J, et al. Sentinel lymph node dissection combined with meticulous histology increases the detection rate of nodal metastases in prostate cancer. Int Urol Nephrol. 2014;46(8):1543–9.
25. Weckermann D, Dorn R, Holl G, Wagner T, Harzmann R. Limitations of radioguided surgery in high-risk prostate cancer. Eur Urol. 2007;51(6):1549–58.
26. Wit EM, Acar C, Grivas N, Yuan C, Horenblas S, Liedberg F, et al. Sentinel node procedure in prostate cancer: a systematic review to assess diagnostic accuracy. Eur Urol. 2016.
27. Manny TB, Patel M, Hemal AK. Fluorescence-enhanced robotic radical prostatectomy using real-time lymphangiography and tissue marking with percutaneous injection of unconjugated indocyanine green: the initial clinical experience in 50 patients. Eur Urol. 2014;65(6):1162–8.
28. Jeschke S, Lusuardi L, Myatt A, Hruby S, Pirich C, Janetschek G. Visualisation of the lymph node pathway in real time by laparoscopic radioisotope- and fluorescence-guided sentinel lymph node dissection in prostate cancer staging. Urology. 2012;80(5):1080–7.
29. Hruby S, Englberger C, Lusuardi L, Schatz T, Kunit T, Abdel-Aal AM, et al. Fluorescence guided targeted pelvic lymph node dissection for intermediate and high risk prostate cancer. J Urol. 2015;194(2):357–63.
30. Yuen K, Miura T, Sakai I, Kiyosue A, Yamashita M. Intraoperative fluorescence imaging for detection of sentinel lymph nodes and lymphatic vessels during open prostatectomy using indocyanine green. J Urol. 2015;194(2):371–7.
31. Miki J, Yanagisawa T, Tsuzuki S, Mori K, Urabe F, Kayano S, et al. Anatomical localization and clinical impact of sentinel lymph nodes based on patterns of pelvic lymphatic drainage in clinically localized prostate cancer. Prostate. 2018;78(6):419–25.
32. Nguyen DP, Huber PM, Metzger TA, Genitsch V, Schudel HH, Thalmann GN. A specific mapping study using fluorescence sentinel lymph node detection in patients with intermediate- and high-risk prostate cancer undergoing extended pelvic lymph node dissection. Eur Urol. 2016;70(5):734–7.
33. Aoun F, Albisinni S, Zanaty M, Hassan T, Janetschek G, van Velthoven R. Indocyanine green fluorescence-guided sentinel lymph node identification in urologic cancers: a systematic review and meta-analysis. Minerva urologica e nefrologica = The Italian Journal of Urology and Nephrology. 2018;70(4):361–9.
34. van Leeuwen AC, Buckle T, Bendle G, Vermeeren L, Valdes Olmos R, van de Poel HG, et al. Tracer-cocktail injections for combined pre- and intraoperative multimodal imaging of lymph nodes in a spontaneous mouse prostate tumor model. J Biomed Opt. 2011;16(1): 016004.
35. KleinJan GH, van den Berg NS, Brouwer OR, de Jong J, Acar C, Wit EM, et al. Optimisation of fluorescence guidance during robot-assisted laparoscopic sentinel node biopsy for prostate cancer. Eur Urol. 2014;66(6):991–8.
36. Dindo D, Demartines N, Clavien PA. Classification of surgical complications: a new proposal with evaluation in a cohort of 6336 patients and results of a survey. Ann Surg. 2004;240(2):205–13.
37. Gharzai LA, Jiang R, Wallington D, Jones G, Birer S, Jairath N, et al. Intermediate clinical endpoints for surrogacy in localised prostate cancer: an aggregate meta-analysis. Lancet Oncol. 2021;22(3):402–10.
38. KleinJan GH, van den Berg NS, de Jong J, Wit EM, Thygessen H, Vegt E, et al. Multimodal hybrid imaging agents for sentinel node mapping as a means to (re)connect nuclear medicine to advances made in robot-assisted surgery. Eur J Nucl Med Mol Imaging. 2016;43(7):1278–87.
39. Brouwer OR, Buckle T, Vermeeren L, Klop WM, Balm AJ, van der Poel HG, et al. Comparing the hybrid fluorescent-radioactive tracer indocyanine green-99mTc-nanocolloid with 99mTc-nanocolloid for sentinel node identification: a validation study using lymphoscintigraphy and SPECT/CT. J Nucl Med Off Publ Soc Nucl Med. 2012;53(7):1034–40.

40. Luhrs O, Ekdahl L, Lonnerfors C, Geppert B, Persson J. Combining Indocyanine Green and Tc(99)-nanocolloid does not increase the detection rate of sentinel lymph nodes in early stage cervical cancer compared to Indocyanine Green alone. Gynecol Oncol. 2020;156(2):335–40.
41. Soergel P, Kirschke J, Klapdor R, Derlin T, Hillemanns P, Hertel H. Sentinel lymphadenectomy in cervical cancer using near infrared fluorescence from indocyanine green combined with technetium-99m-nanocolloid. Lasers Surg Med. 2018;50(10):994–1001.
42. Rundle S, Korompelis P, Ralte A, Bewick D, Ratnavelu N. A comparison of ICG-NIR with blue dye and technetium for the detection of sentinel lymph nodes in vulvar cancer. Eur J Surg Oncol. 2023; 49(2):481–485
43. Azargoshasb S, Boekestijn I, Roestenberg M, KleinJan GH, van der Hage JA, van der Poel HG, et al. Quantifying the impact of signal-to-background ratios on surgical discrimination of fluorescent lesions. Mol Imaging Biol. 2022.
44. Meershoek P, KleinJan GH, van Willigen DM, Bauwens KP, Spa SJ, van Beurden F, et al. Multi-wavelength fluorescence imaging with a da Vinci Firefly-a technical look behind the scenes. J Robot Surg. 2021;15(5):751–60.
45. KleinJan GH, Van Den Berg NS, Brouwer OR, Acar C, Wit EM, Vegt E, et al. Improving fluorescence-guided sentinel node detection during robot-assisted laparoscopic sentinel node biopsy for prostate cancer. Eur J Nucl Med Mol Imaging. 2014;41:S288.
46. Meershoek P, Buckle T, van Oosterom MN, KleinJan GH, van der Poel HG, van Leeuwen FWB. Can intraoperative fluorescence imaging identify all lesions while the road map created by preoperative nuclear imaging is masked? J Nucl Med Off Publ Soc Nucl Med. 2020;61(6):834–41.
47. Hensbergen AW, van Willigen DM, van Beurden F, van Leeuwen PJ, Buckle T, Schottelius M, et al. Image-guided surgery: are we getting the most out of small-molecule prostate-specific-membrane-antigen-targeted tracers? Bioconjug Chem. 2020;31(2):375–95.
48. Vidal-Sicart S, Valdes Olmos RA. Sentinel node approach in prostate cancer. Rev Esp Med Nucl Imagen Mol. 2015;34(6):358–71.
49. Dell'Oglio P, Meershoek P, Maurer T, Wit EMK, van Leeuwen PJ, van der Poel HG, et al. A DROP-IN gamma probe for robot-assisted radioguided surgery of lymph nodes during radical prostatectomy. Eur Urol. 2021;79(1):124–32.
50. Brausi M, Hoskin P, Andritsch E, Banks I, Beishon M, Boyle H, et al. ECCO essential requirements for quality cancer care: prostate cancer. Crit Rev Oncol Hematol. 2020;148: 102861.
51. Wit EMK, van Beurden F, Kleinjan GH, Grivas N, de Korne CM, Buckle T, et al. The impact of drainage pathways on the detection of nodal metastases in prostate cancer: a phase II randomized comparison of intratumoral vs intraprostatic tracer injection for sentinel node detection. Eur J Nucl Med Mol Imaging. 2022;49(5):1743–53.

Authors and Affiliations

Esther M. K. Wit[1] · Gijs H. KleinJan[1,2,3] · Anne-Claire Berrens[1] · Roos van Vliet[1] · Pim J. van Leeuwen[1] · Tessa Buckle[1,2] · Maarten L. Donswijk[4] · Elise M. Bekers[5] · Fijs W. B. van Leeuwen[1,2] · Henk G. van der Poel[1,6]

[1] Department of Urology, The Netherlands Cancer Institute – Antoni van Leeuwenhoek Hospital, Plesmanlaan 121, 1066 CX Amsterdam, The Netherlands

[2] Interventional Molecular Imaging Laboratory, Department of Radiology, Leiden University Medical Center, Leiden, The Netherlands

[3] Department of Urology, Leiden University Medical Center, Leiden, The Netherlands

[4] Department of Nuclear Medicine, The Netherlands Cancer Institute – Antoni van Leeuwenhoek Hospital, Amsterdam, The Netherlands

[5] Department of Pathology, The Netherlands Cancer Institute – Antoni van Leeuwenhoek Hospital, Amsterdam, The Netherlands

[6] Department of Urology, Amsterdam University Medical Center, Amsterdam, The Netherlands